Image reconstruction from linear attenuating operators

Mila Nikolova

CMLA, ENS Cachan, CNRS, France

The 8th International Congress on Industrial and Applied Mathematics (ICIAM 15)

10-14 August 2015, Beijing, China

Acknowledgements

We thank Eric Vourc'h (SATIE, ENS Cachan) for helpful discussions and sharing data

Sponsor of work presented here:

Institut Farman FR 3311 – Project INVERSYM 2

1. Introduction

Data acquisition in some imaging systems is modeled using linear attenuating operators

(e.g., ultra-sound testing in through-transmission, electron paramagnetic resonance testing, ECT)

Eddy current testing (ECT) for nondestructive evaluation

- Detect and characterize flaws in conductive materials using electromagnetic induction

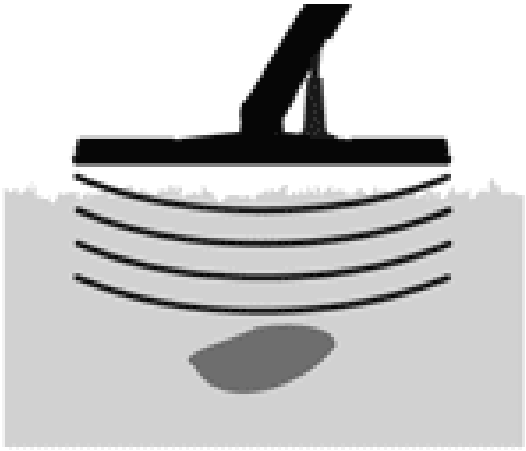

1. Detector transmits an electromagnetic field

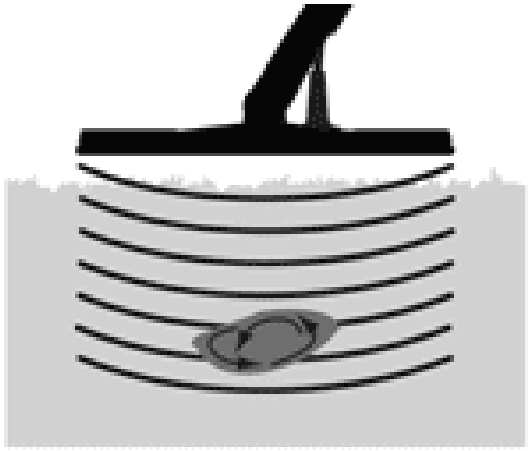

2. Eddy currents are induced into the target

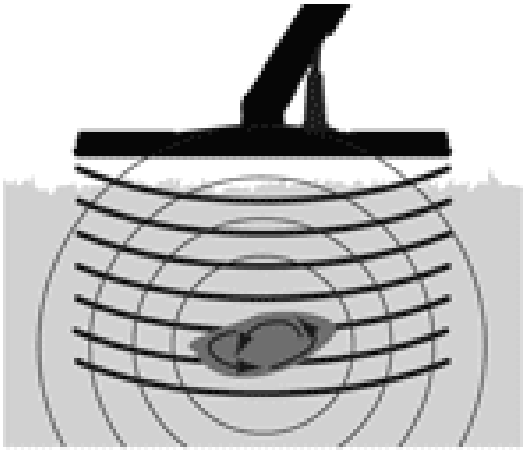

3. Eddy currents generate an electromagnetic field

- ECT as a technique was discovered unintentionally by Hans Christian Oersted in 1820
- ECT for industrial applications – World War II (Germany)
- Multi-frequency testing introduced in 1974 (France)

Data acquisition

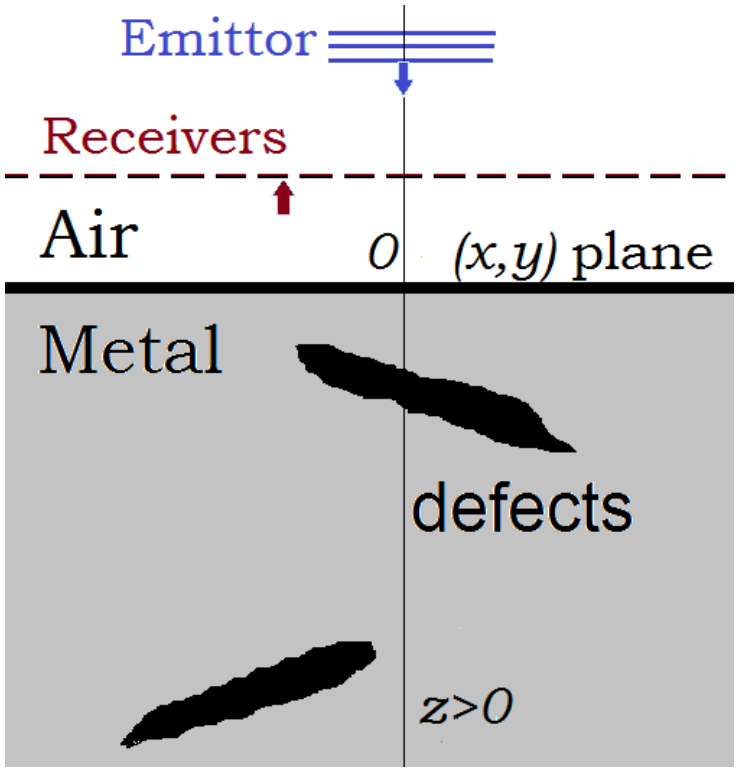

(b)

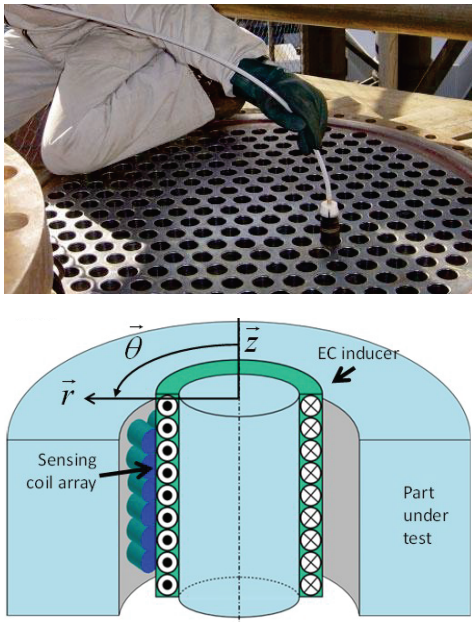

(c)

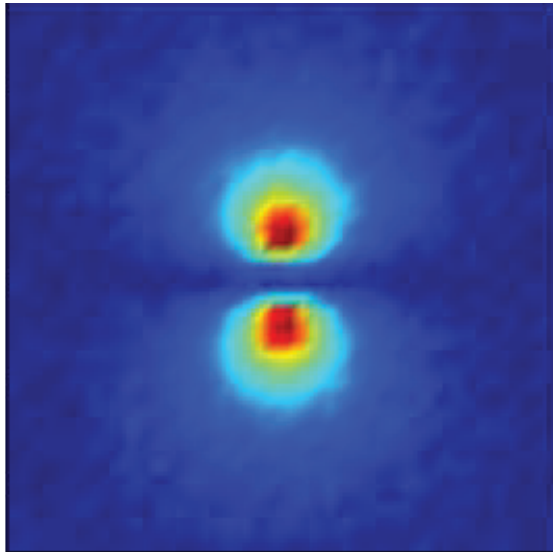

Measures: $d(x, y; \nu)$ magnetic flux for frequency ν

Image credits to E. Vourc'h for (b) and (c)

Some fields of application:

aeronautics, nuclear industry, steel industry, motor industry, petroleum engineering

Advantages:

easy to apply, no contact with the material, no pollution, safe, very cheap

- Pessimism about ECT in the 1980s – difficult to check that workers really did the job
  (An alternative – Magnetic particle Inspection – but more constraints than ECT)
- A lot of progress in research on ECT – industrials came back again (2012) lots of expectation

Main open problems:

- Improve the theoretical modeling in different configurations
- 3D image reconstruction and rigorous validation
- Subsurface reconstruction limit due to the skin effect = attenuation with the depth

A general forward model

$$d_\nu = A_\nu \breve{u} + \text{noise}$$

$\breve{u} \in \{0, 1\}$ – the inspected material

$\nu \in \{\nu_1, \ldots, \nu_k\}$ a set of frequencies

A_ν – the observation operator for ν (ill-conditioned)

A_ν has a particular structure:

$$A_\nu = G_\nu H_\nu \qquad H_\nu = \mathrm{diag}\{e^{-\lambda_\nu z}\}$$

H_ν – skin effect – (vertical attenuation)

Each layer z is multiplied by $e^{-\lambda_\nu z}$ $\Longrightarrow$

a stiff degradation of the representation of different layers into the data

Skin effect + noise – the major difficulty in ECT image reconstruction

Challenge: to increase the depth of inspection

Dealing with attenuation under noise is the core of our talk

2. Our variational approach

The sought image $\hat{u} \in \mathbb{R}^{M \times N}$ should estimate the location and the geometry of defects

$$\hat{u} = \arg\min_{u \in S} \left\{ J(u) = \Psi(u; d) + \beta \Phi(u) \right\}$$

- $\hat{u}$ should be piecewise constant $\quad \Rightarrow \quad$ $\Phi \sim$ TV-like to promote stair-casing

$$\Psi(u) = \mathrm{TV}_\gamma(u) := \sum_i \sum_j \gamma_{ij} |(\nabla u)_{ij}| \qquad |(\nabla u)_{ij}| := \sqrt{(\nabla_y u)_{ij}^2 + (\nabla_x u)_{ij}^2}$$

  $\mathrm{TV}_1 = \mathrm{TV}$ (Rudin-Osher-Fatemi, 1992)

- The usual choice for data-fidelity term is $\Psi(\cdot) = \frac{1}{2} \| \cdot \|_2^2$

$$J_2(u) := \frac{1}{2} \|Au - d\|_2^2 + \beta \mathrm{TV}_\gamma(u)$$

- $\ell_1 - \mathrm{TV}$ criteria, where $\Psi(\cdot) = \| \cdot \|_1$, give rise to more geometric solutions

$$J_1(u) := \|Au - d\|_1 + \beta \mathrm{TV}_\gamma(u)$$

Our approach: adjust γ to the attenuation H for J_1 and for J_2.

The references on ECT regularization do not consider adjustment to attenuation; e.g.

S. Bausson, V. Thomas, P-Y. Joubert, L. Blanc-Féraud, J. Darbon, G. Aubert, Regularized inversion of a distributed point source model for the reconstruction of defects in eddy currents imaging, COMPEL Vol. 30 No. 6, 2011, pp. 1777–1791.

A. Lopes Ribeiro, H. G. Ramos, D. Pasadas, and T. Rocha, Regularization Methods to Assess the Eddy Current Density Inside Conductive Non-Ferromagnetic Media, AIP Conference Proceedings; 2014, Vol. 1581, pp. 1428–1432

A. Lopes Ribeiro, H. G. Ramos, Exploring the Eddy Current Excitation Invariance to Infer About Defect Characteristics, AIP Conference Proceedings, Vol. 1335 Issue 1, 2011

G. Rubinacci, A. Tamburrino, S. Ventre, Regularization and numerical optimization of a fast eddy current imaging method, Magnetics, IEEE Transactions, 42(4), 2006, pp. 1179–1182

D. Prémel and P. Baussard. Eddy current evaluation of 3D flaws in flat conductive materials using a bayesian approach. Inverse Problems, 2002;18(6), pp. 1873–1889.

These methods provide a resolution that rapidly decays with the depth
Focus on defects located at the surface of the inspected material.

Adaptation to the attenuation

Focus on $\quad d_{kj} = h_k \breve{u}_{kj} + n_{kj} \quad \forall\, j \quad \Longleftrightarrow \quad d = \mathrm{diag}(h)\breve{u} + n$

$1 = h_1 > h_2 > \cdots > h_M > 0$

- $$J_2(u) = \frac{1}{2}\sum_{kj}(h_k u_{kj} - h_k \breve{u}_{kj} + n_{kj})^2 + \beta \sum_{kj} \gamma_k |(\nabla u)_{kj}|$$
$$= \frac{1}{2}\sum_{kj} h_k^2 \left(u_{kj} - \breve{u}_{kj} + \frac{n_{kj}}{h_k}\right)^2 + \beta \sum_{kj} \gamma_k |(\nabla u)_{kj}|$$

  Let $\gamma_k = h_k^2$

$$J_2(u) = \sum_{k=1}^{M} h_k^2 \sum_{j=1}^{N} \left(\left(u_{kj} - \breve{u}_{kj} + \frac{n_{kj}}{h_k}\right)^2 + \beta \left|(\nabla u)_{kj}\right| \right)$$

  $\boldsymbol{\gamma_k := h_k^2}$ for $k = 1, \ldots, L$ so that if $k > L$ the noise may not be smoothed.

- $$J_1(u) = \sum_{kj} h_k \left| u_{kj} - \breve{u}_{kj} + \frac{n_{kj}}{h_k} \right| + \beta \sum_{kj} \gamma_k |(\nabla u)_{kj}|$$

  $\boldsymbol{\gamma_k := h_k}$ for $k = 1, \ldots, L$ so that if $k > L$ the noise may not be smoothed.

$\breve{u} : 110 \times 41 \qquad d = \mathrm{diag}(h)\breve{u} + n \qquad h_k = e^{-\frac{k-1}{25}} \qquad 1 \leq k \leq M$ SNR=22dB

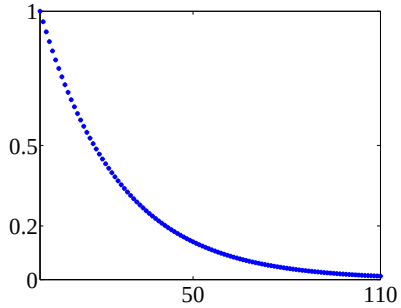

each row k of the input image $\breve{u}$ is multiplied by h_k before adding the noise

$\Rightarrow$ a stiff degradation of the pixel values $(h_1 = 1$ and $h_M = 0.0128)$

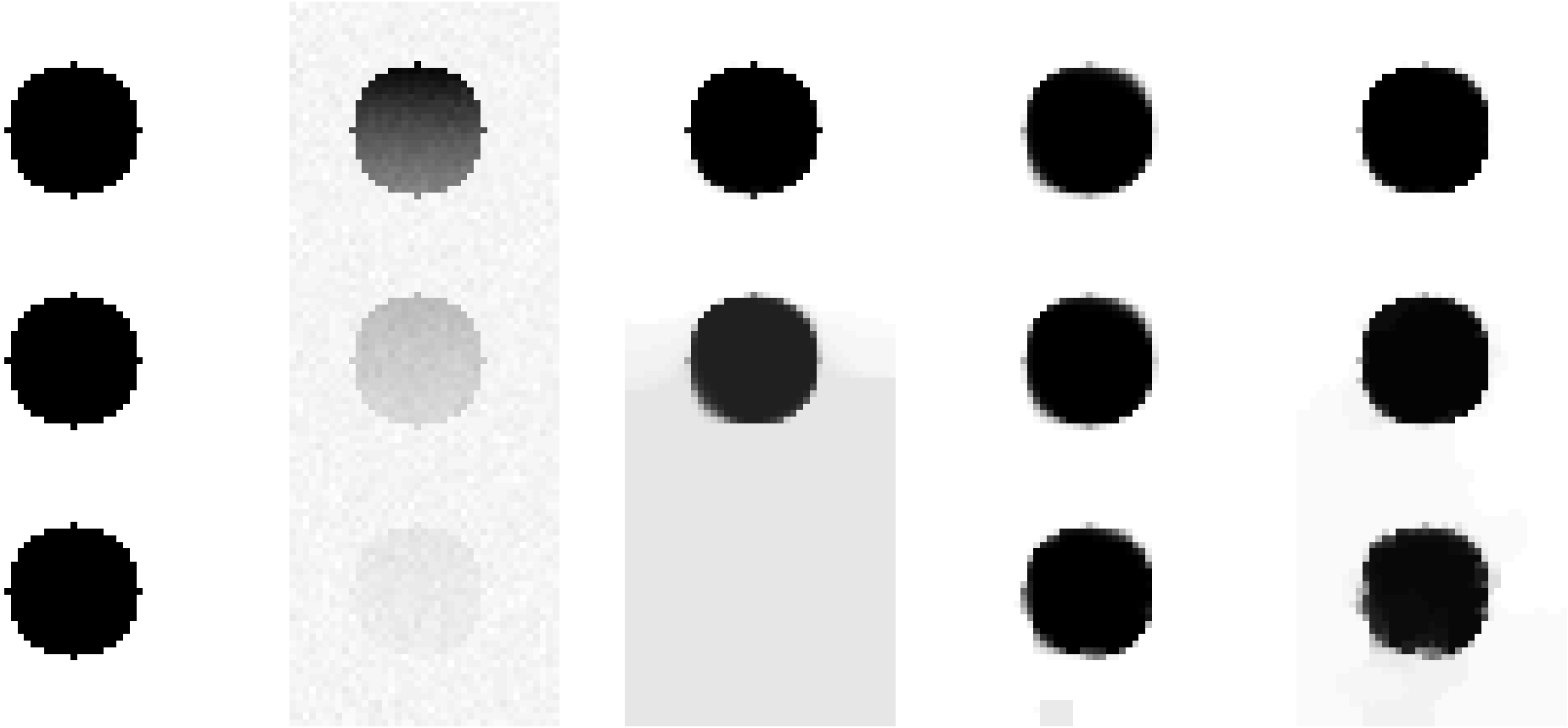

original 110×41 | data d | J_2, $\gamma = 1$ | J_2, $\gamma_k = h_k^2$ | J_1, $\gamma_k = h_k$

Examples on $\mathbb{R}$

$$d = h\breve{u} + n \qquad\qquad h > 0$$

- $J_2(u) = \dfrac{1}{2}(hu - d)^2 + \beta\gamma|u|$

$$\hat{u} = \min\left\{0,\ \frac{|d|}{h} - \frac{\beta\gamma}{h^2}\right\}\operatorname{sign}(d)$$

Let $d > 0$

$$\hat{u} = \min\left\{0,\ \breve{u} + \frac{n}{h} - \frac{\beta\gamma}{h^2}\right\}$$

- $J_1(u) = |hu - d| + \beta\gamma|u|$

$$\hat{u} = \frac{d}{h}\,\mathbb{1}(\beta\gamma < h) = \left(\breve{u} + \frac{n}{h}\right)\,\mathbb{1}(\beta\gamma < h)$$

- The sought-after images are piece-wise constant.

  The denoising of constant parts is due to the stair-case implied by the regularization.

Extension to attenuating operators $A = GH$

The exhibited values of γ when $A = \mathrm{diag}(h)$ with $\{h_k\}$ strictly decreasing (attenuation) are applied to $A = GH = G\mathrm{diag}(h)$

This is exact for J_2 if $G^*G = I$

For A attenuating (up to down the image) one can extract a decomposition $A = G\mathrm{diag}(h)$

Our approach can be generalized to other observation operators involving stiff degradation of the pixel values

degraded restored

Known shading and blur

3. Saddle-point formulation

The main ingredients are obtained using the "dual transportation trick"

Let $u \in X = \mathbb{R}^{M\times N}$, $\nabla u \in Y = (X, X)$ and $d \in Z$

- Data-fidelity terms for $Z(\mathbb{R})$

$$\frac{1}{2}\|Au - d\|_2^2 = \sup_{v\in Z} \langle v, Au - d\rangle - \frac{1}{2}\|v\|^2$$

$$\|Au - d\|_1 = \sup_{v\in Z} \langle v, Au - d\rangle - \delta_{B_\infty}(v) \qquad B_\infty := \{v \in Z \ : \ \|v\|_\infty \leq 1\}$$

- Data-fidelity terms for $Z(\mathbb{C}) \sim Z(\mathbb{R}) \times Z(\mathbb{R})$

$$\frac{1}{2}\|Au - d\|_2^2 = \max_{v\in Z} \left(\langle v, \Re(Au - d)\rangle - \frac{1}{2}\|v\|^2 \right) + \max_{w\in Z} \left(\langle w, \Im(Au - d)\rangle - \frac{1}{2}\|w\|^2 \right)$$

$$\|Au - d\|_1 = \max_{(v,w)\in(Z\times Z)} \langle v, \Re(Au - d)\rangle + \langle w, \Im(Au - d)\rangle - \delta_{B_{2,\infty}}(v, w)$$

$$B_{2,\infty} := \left\{ v = (v', v'') \in Z \times Z \ : \ \|v\|_\infty := \max_{ij} \sqrt{(v'_{i,j})^2 + (v''_{i,j})^2} \leq 1 \quad \forall\, (i, j) \right\}$$

- Regularization

$$\mathrm{TV}_\gamma := \sum_{ij} \gamma_{ij} |(\nabla u)_{ij}| = \sup_{p\in Y} \langle p, \nabla u\rangle - \delta_{P^\gamma_{2,\infty}}(p)$$

$$P^\gamma_{2,\infty} := \left\{ p \in Y \ : \ \|p_{i,j}\|_2 = \sqrt{(p'_{i,j})^2 + (p''_{i,j})^2} \leq \gamma_{ij} \quad \forall\, (i, j) \right\}$$

- Box constraints are easily incorporated

Equivalent formulations for J_1 and J_2

$$\begin{aligned}\arg\min_{u\in B_\infty} J_2(u) &= \arg\min_u \max_p \frac{1}{2}\|Au-d\|_2^2 + \beta\langle p, \nabla u\rangle - \delta_{P_{2,\infty}^\gamma}(p) + \delta_{B_\infty}(u) \\ &= \arg\min_u \max_p \max_v \langle v, Au-d\rangle - \frac{1}{2}\|v\|^2 + \beta\langle p, \nabla u\rangle - \delta_{P_{2,\infty}^\gamma}(p) + \delta_{B_\infty}(u)\end{aligned}$$

$$\arg\min_{u\in B_\infty} J_1(u) = \arg\min_u \max_p \max_v \langle v, Au-d\rangle - \delta_{B_\infty}(v) + \beta\langle p, \nabla u\rangle - \delta_{P_{2,\infty}^\gamma}(p) + \delta_{B_\infty}(u)$$

Similar formulations for data-fidelity on $Z(\mathbb{C})$

Algorithms: PAPC [Driori, Sabach, Teboulle 15] for J_2 and primal-dual [Chambolle-Pock 11]

Solving equivalently $\arg\min_{u\in S}\left\{\frac{1}{\beta}\Psi(u;d) + \Phi(u)\right\}$ is sometimes faster

4. Numerical tests

In NDE false alarms are safer than non detection

Convolution with attenuation and noise

$\breve{u} : 100 \times 31 \qquad d = a * \mathrm{diag}(h)\breve{u} + n \qquad h_k = e^{-0.04(k-1)}, \quad 1 \le k \le M \qquad (h_M = 0.0191)$

PSF a – circle, $\mathrm{diam}(a) = 7$ pix., Gaussian noise, SNR $= 24$ dB

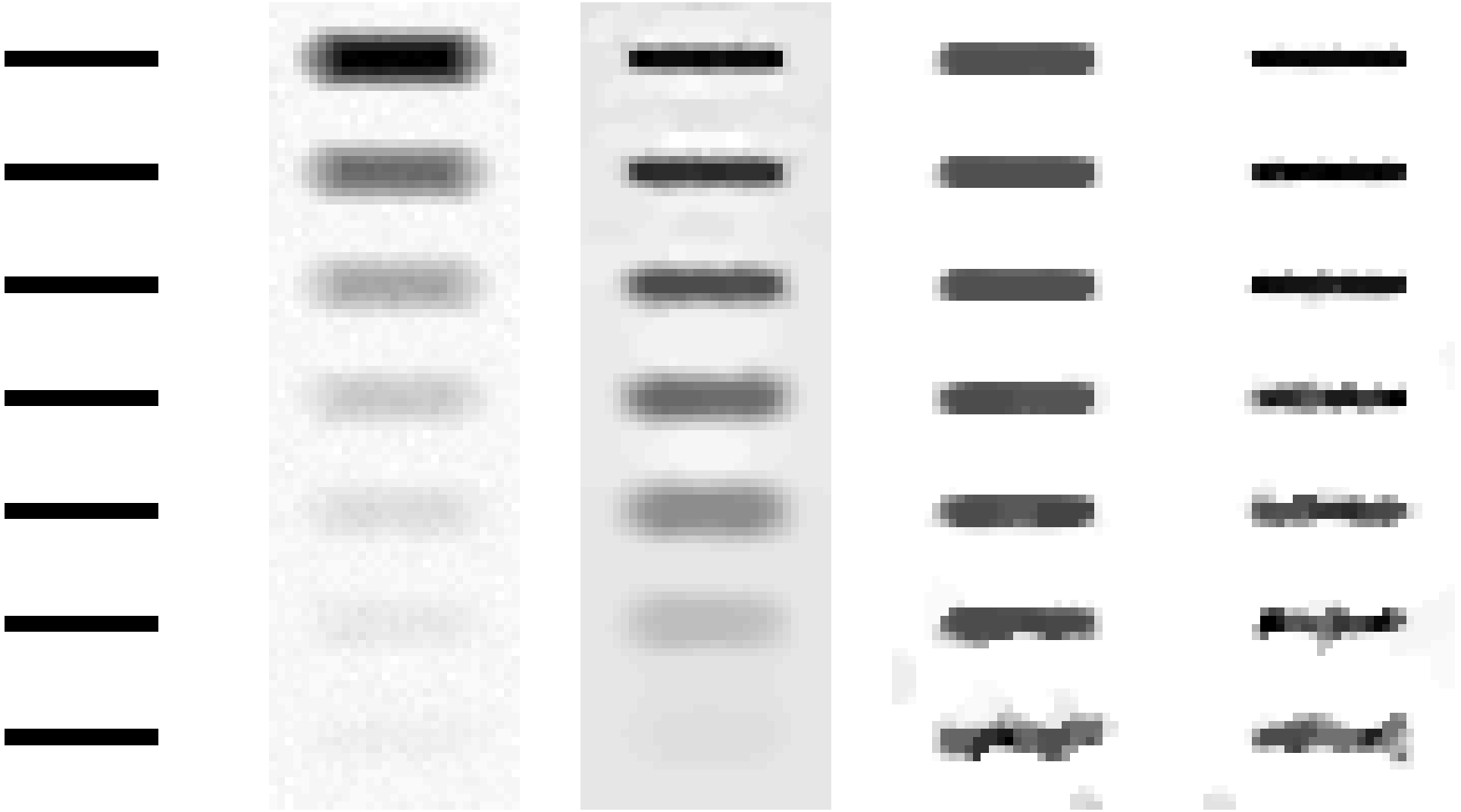

original 100×31 | data d | $J_2,\ \gamma = 1$ | $J_2,\ \gamma_k = h_k^2$ | $J_1,\ \gamma_k = h_k$

Noise-free data

$\breve{u} : 100 \times 31 \qquad d = a * \mathrm{diag}(h)\breve{u} \qquad h_k = e^{-0.04(k-1)}, \quad 1 \le k \le M \qquad$ (no noise)

$\breve{u}\ 100 \times 31$ | data: d | $J_2,\ \gamma = 1$ | $J_2,\ \gamma_k = h_k^2$ | $J_1,\ \gamma_k = h_k$

$\{\gamma_k\}$ as proposed $\Longrightarrow$ no attenuation in the reconstructed images

Noisy Fourier-Laplace data (one of the models for ECT)

$\breve{u} \in \mathbb{R}^{182\times 90}$ $\quad d = \mathrm{fft2}\big(\mathrm{diag}(h)\breve{u}\big) + n$ $\qquad h_k = e^{-0.03(k-1)}, \quad 1 \le k \le M \quad h_M = 0.0044$

SNR$= 19$ dB

original 182×90

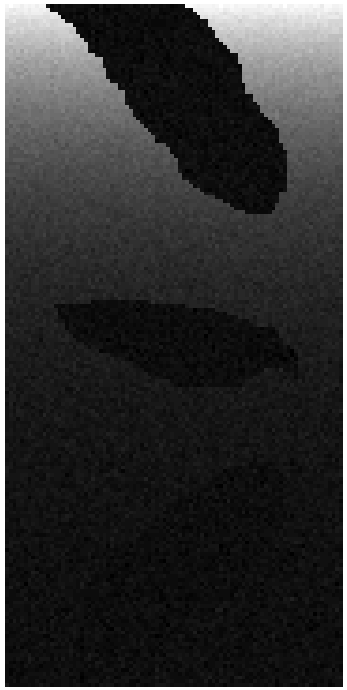

$\Re(\mathrm{ifft2}(d))$

$J_2,\ \gamma = 1$

$J_2,\ \gamma_k = h_k^2$

$J_1,\ \gamma_k = h_k$

5. Conclusions and open questions

- When A is a stiff attenuating observation operator, the regularization weights have to be properly adjusted to each attenuation level.
- This fact is independent of nature of the noise.
- The adjustment of the regularization weights depends on the whole objective function.

- We have derived regularization weights $\{\gamma_k\}$ based only on the attenuation operator (corresponding to the skin effect in eddy current testing)

  They might be improved by considering the whole operator $A = GH$.
- The ℓ_1 based objective function J_1 seems to provide more precise results.
- The interplay between β and $\{\gamma_k\}$ according to the noise needs clarification.
- The limit L of the adjustment $\{\gamma_k\}_{k=1}^{L}$ has to be explored according to the noise.
- The extension to 3D objects does not present substantial difficulties.

Thank you for your attention!

Thanks to the Organizers of the Mini symposium for the invitation !